INTRACTION OF LASER RADIATION WITH MATTER. LASER PLASMA PACS numbers: 52.38.Mf; 42.68.Mj
DOI: 10.1070/QE2002v032n05ABEH002213

Effect of nonlinear light scattering in air on ablation of materials produced by femtosecond laser pulses

S.M. Klimentov, T.V. Kononenko, P.A. Pivovarov, V.I. Konov, A.M. Prokhorov, D. Breitling, F. Dausinger

***Abstract*. Nonlinear light scattering appearing upon air breakdown induced by high-power ultrashort pulses (110–5200 fs) from a Ti : Al_2O_3 laser is studied. As a result of forward scattering, the beam profile is severely deformed, which is accompanied by spectral conversion of the incident radiation to a series of shorter-wavelength peaks extending into the visible spectral range. Measurements are made of the thresholds and the scattered radiation energy, which amounts to 75 % of the incident energy. The effect of scattering on the material ablation in air is investigated. The obtained data offer an explanation for the experimentally observed paradoxical morphology of the channels ablated by high-power femtosecond pulses.**

Keywords: *ablation, femtosecond laser pulses, nonlinear scattering, laser plasma.*

1. Introduction

Our work is concerned with the study of the effect of a gas medium on the ablation produced by ultrashort laser pulses, including the formation of deep channels. As is known, the use of the femtosecond laser pulses for material microprocessing involves expectations to enable an efficient and high-precision action of radiation on a material. These advantages may be realised due to small dimensions of the region of thermal action, which approach the diffraction limit upon the radiation focusing [1–3]. However, a significant growth of the region of thermal influence upon the ablation of materials by high-power short radiation pulses may result from the production and radial expansion of a plasma plume after ultrashort-pulse laser irradiation [4] and also from the optical breakdown of the gas medium in which the irradiation is performed.

As shown in Ref. [5], the presence of air during the ablation formation of deep channels by picosecond pulses results in the production of a long-lived ablated-particle suspension and in the low-threshold air breakdown at these particles. This has a dramatic effect on the rate and results of the processing. This type of ambient screening effect was noted to occur despite the fact that the breakdown thresholds for picosecond pulses in pure air are very high.

As the duration τ of irradiation pulses shortens to subpicoseconds, the threshold for the optical breakdown in pure air lowers significantly. In this case, however, the breakdown plasma exerts a significantly weaker effect on the incident energy [5]. Upon irradiation by such subpicosecond pulses, one would expect the prevalence of processes responsible for a strong radiation self-action and scattering, including the nonlinear scattering [6–9]. To simulate the material ablation produced by intense ultrashort pulses in the ambient air, we study in this paper the characteristics of such scattering in the air breakdown plasma without a target and then consider its possible effect on the morphology of channels produced in steel.

2. Experimental

Experiments on material ablation and the recording of scattered radiation were performed in air using a 'Hurricane' Ti : Al_2O_3 laser (Spectra-Physics) with a pulse repetition rate of 1 kHz for a pulse duration from 100 fs to 5 ps. The laser beam with a spatial profile close to a Gaussian was focused with a long-focus lens to a beam waist 18 μm in diameter at the $1/e^2$ intensity level. In accordance with the scheme shown in Fig. 1, the scattering measurements involved the recording of radiation parameters behind the beam waist as functions of the energy and the laser pulse duration.

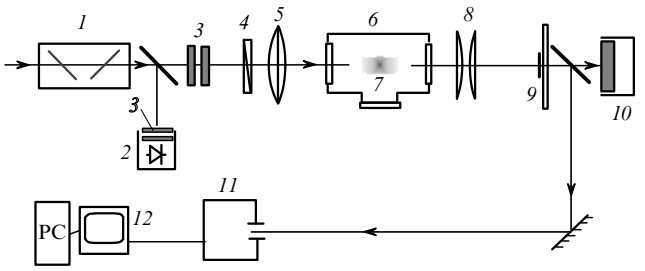

Figure 1. Scheme of the setup for recording forward radiation scattering: (*1*) attenuator; (*2*) power meter; (*3*) neutral-density optical attenuation filters; (*4*) $\lambda/4$ plate; (*5*) focusing lens; (*6*) vacuum chamber; (*7*) laser-produced spark; (*8*) condenser; (*9*) reflecting screen; (*10*) wide-aperture power meter; (*11*) spectrometer; (*12*) computer.

S.M. Klimentov, T.V. Kononenko, P.A. Pivovarov, V.I. Konov, A.M. Prokhorov Institute of General Physics, Russian Academy of Sciences, ul. Vavilova 38, 119991 Moscow, Russia; fax: (095) 135 76 72; e-mail: kliment@kapella.gpi.ru;
D. Breitling, F. Dausinger Institut für Strahlwerkzeuge, Pfaffenwaldring 43, D-70569 Stuttgart, Germany; fax: 49-0711/6856842

Received 14 January 2002
Kvantovaya Elektronika **32** (5) 433–436 (2002)
Translated by E.N. Ragozin

One part of the transmitted radiation was directed to an automated spectrometer having a temporal resolution of ~ 10 ns and the other arrived at a 'spectrally grey' large-aperture power meter. The forward-scattered part of the radiation was selected with the help of a round reflecting screen, which was glued on a flat glass plate and placed in front of the power meter. The screen diameter was selected in such a way as to block $\sim 90\,\%$ of the energy of the Gaussian beam undistorted by scattering. The appearance of forward scattering resulted in an increase in the fraction of radiation energy passed behind the screen, and a comparison of the energies measured with and without the screen allowed us to judge the degree of screening and energy of forward-scattered radiation. The power meter and the collimating lens could be replaced with a screen or a CCD camera for observing and measuring the profile of transmitted radiation.

The morphology of channels produced in steel upon ablation by femtosecond pulses was investigated by electron microscopy of high-precision longitudinal sections to be subsequently compared with experimental scattering data.

3. Results and discussion

The nonlinear scattering of femtosecond pulses in air is easy to observe on a luminescent screen placed behind the beam waist. Beginning with some threshold energy, the screen revealed a deformation of the initial Gaussian beam profile with the formation of concentric rings. The photograph in Fig. 2 illustrates the appearance of the first such ring. As the energy is further increased the ring structure becomes more complicated, and the radiation in the visible spectral range appears at its periphery.

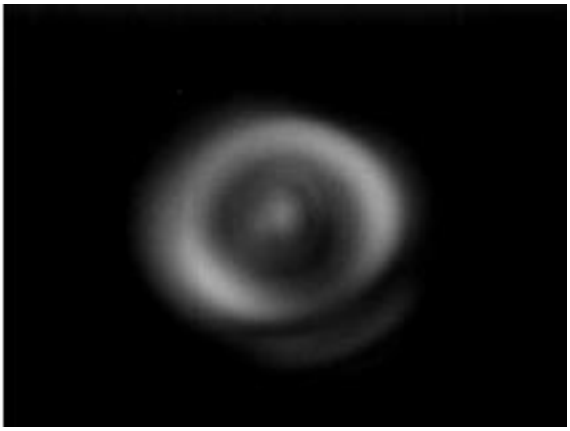

Figure 2. Spatial radiation profile behind the laser spark ($\tau = 110$ fs, 80 J cm^{-2}).

The transmitted and scattered radiation spectra are shown in Fig. 3 for different intensities and durations of laser pulses. The spectra were recorded for a minimal time of exposure of the electronic spectrometer gate equal to 10 ns. In this case, shifting the instant of its operation also by 10 ns from the instant of arrival of a laser pulse resulted in the disappearance of the spectrum. So strict a timing of the measured spectrum probably suggests that the generation of new spectral components occurs during the action of a laser pulse. Recording incident and transmitted radiation pulses with the help of fast photodiodes enabled this time interval to be reduced to ~ 1 ns. Note for comparison that the glow duration of the air breakdown plasma measured under the same conditions was considerably longer than 1 ns, and individual spectral components of the plasma radiation could be recorded more than 100 ns later.

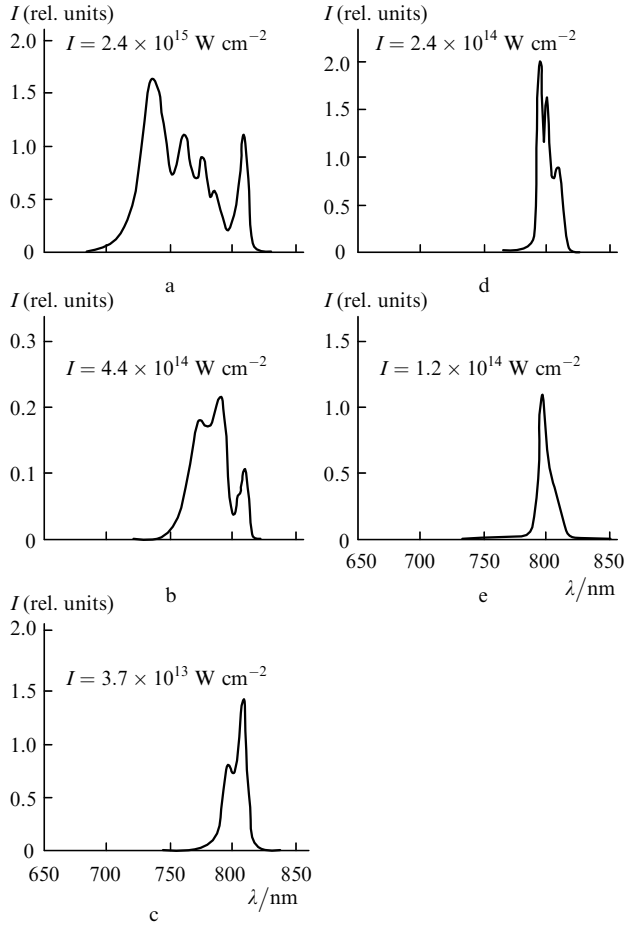

Figure 3. Emission spectra behind the beam waist for different intensities for 110-fs (a – c) and 1100-fs (d – e) laser pulses.

The measured spectra of transmitted radiation (Fig. 3) consist of a series of distinct peaks, the longest-wavelength peak corresponding to the emission band of the femtosecond laser. The number of short-wavelength peaks increases with increasing energy and shortening of radiation pulses and amounts to four or five for the maximum attainable parameters of laser radiation (0.75 mJ, $\tau = 100$ fs). In the experiment we observed no conversion of incident radiation to the longer-wavelength side of the spectrum. Note that the amplitudes of the spectral peaks of scattered radiation shown in Fig. 3 do not quite adequately represent the energy ratio between the spectral components, while the radiation at the fundamental frequency is reduced several-fold compared to other spectral components. The spectrum of scattered light almost does not change when the circularly polarised incident radiation is used.

Blocking the Gaussian spatial component of the beams by the reflecting screen allowed us to measure the scattered-radiation fraction as a function of the energy density and laser-pulse duration. Fig. 4 shows a family of shuch curves

measured in the femtosecond and picosecond ranges. The shortest pulses are characterised by a sharp and very low energy threshold, a rapid build-up of the scattered energy, and the onset of saturation on reaching an energy density of 50 – 100 J cm^{-2}. The longest picosecond pulses in the series, on the other hand, are characterised by an almost linear build-up of scattered radiation energy. In the middle of the duration range attainable in the experiments there supposedly occurs a change of the scattering mechanism, and the combined action of the two mechanisms in the transition range corresponds to the maximum scattering coefficient (up to 75 % for $\tau \approx 1100$ fs) for the maximum incident energy.

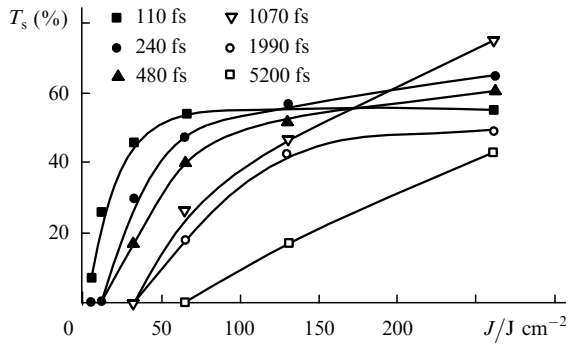

Figure 4. Scattered-radiation fraction versus the energy density for different laser pulse durations τ.

The dependence of energy scattering threshold on the laser-pulse duration τ was determined employing different criteria, including the scattered radiation energy, beam profile deformation, and the occurrence of new spectral components in the forward-scattered radiation. Also shown for comparison here are the thresholds for the initiation of a visible spark in air. One can see from Fig. 5, which illustrates the results of these measurements, that the threshold intensity begins to increase sharply for laser pulse durations $\tau < 1 - 2$ ps. However, the threshold in energy density, which is determined by extrapolating the curves in Fig. 4, continues to decrease, achieving 4 – 6 J cm^{-2} for $\tau = 110$ fs.

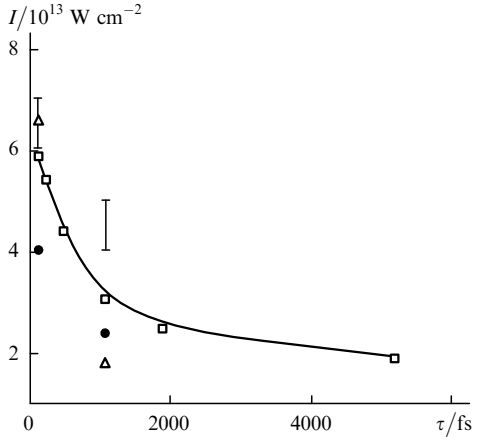

Figure 5. Intensity scattering thresholds as functions of the laser pulse duration. The thresholds are determined using different criteria: the energy of scattered radiation (□), the occurrence of new spectral components (●), and the deformation of the beam profile (Ī). In the latter case, the lower boundary of a range corresponds to the onset of deformation of the Gaussian distribution and the upper one corresponds to the appearance of the first ring. The thresholds for the initiation of a visible spark in air are shown for comparison (△).

When examining Fig. 5, it is interesting to compare the order in which the above features or criteria reveal themselves. In the short-duration range, the spectral radiation conversion and the deformation of the beam profile are observed first with increasing radiation intensity, but a significantly higher energy is required for the origination of a visible laser-induced plasma. At the same time, the appearance of a plasma spark in the transition region ($\tau = 1 - 2$ ps) is the most sensitive forerunner of the scattering, and the spectral conversion related to the nonlinear light scattering has a higher threshold. This indicates to the possible coexistence of two scattering mechanisms for pulse durations of the order of several picoseconds. One of them is engaged when the spatial extent of an ultrashort pulse exceeds the longitudinal dimension of the focal region. The other, the faster one, does not necessitate the presence of a plasma or is realised at the earliest stage of its production.

Clearly, the scattering of so large a fraction of the energy of femtosecond pulses will necessarily tell on the results of material ablation in air. It is the deformation of spatial beam profile with the formation of a ring system that is the main cause for the increase in diameter of the holes produces by ablation in steel [5]. It is also the cause for the emergence of a paradoxical, at the first glance, bottom and wall relief of the channels, as illustrated by the series of longitudinal channel sections shown in Fig. 6. The distinct annular structures at the periphery of the microsections of holes shown in Fig. 6 clearly confirm this assumption.

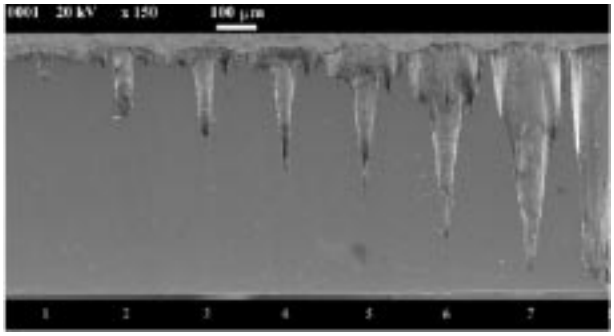

Figure 6. Longitudinal sections of the channels in steel produced by laser ablation with 130-fs pulses for the energy density 250 J cm^{-2}.

This becomes all the more evident because, according to the data of Fig. 5, the laser beam region in which the energy density exceeds the threshold for profile deformation with the occurrence of an annular spatial distribution (6 – 10 J cm^{-2}) should be rather distant from the beam waist plane. On the one hand, the very narrow and deep peaks of surface relief, which are distinct in Fig. 6 are not smoothed by plasma flow and can only result from a direct irradiation of the material by a laser beam with a substantially nonuniform profile. On the other hand, the possible influence of diffraction involving reflections from the walls can be ruled out in this case because the annular relief emerges even at the initial stages of channel production.

4. Conclusions

We have observed a strong coherent forward scattering upon focusing ablation femtosecond pulses in air. The scattering is accompanied by an efficient spectral radiation conversion with the emergence of a series of short-wavelength peaks and a beam profile distortion with the occurrence of an annular structure. We assume the existence of two mechanisms of scattering of high-intensity laser beams in air upon irradiation by 0.1 – 5-ps pulses. One of them may be due to the appearance of self-phase modulation or SRS [8] and the other may be caused by the inhomogeneity of air breakdown plasma or self-focusing [6, 7, 9]. The former scattering mechanism is most pronounced in the subpicosecond range, while in the few-picosecond range both mechanisms act simultaneously. A more detailed elucidation of the balance and nature of these mechanisms invites further investigation.

Due to the high efficiency of forward scattering, the beam profile deformation has catastrophic consequences for ablation results, causing a many-fold increase in diameters of the channels being produced and resulting in the emergence of a complex nonuniform relief of the bottom and of the walls. The change of the emission spectrum caused by this scattering should be taken into account when constructing theoretical models of the interaction of intense ablation femtosecond pulses with materials, particularly semiconductors and dielectrics.

Acknowledgements. This work was supported by the PRIMUS Programme and the Russian Foundation for Basic Research (Grant No. 00-02-17535). The authors thank S.V. Garnov and A.A. Malyutin for useful discussion of the results.

References

1. Preuss S., Demchuk A., Stuke M. *Appl. Phys. A*, **61**, 33 (1995).
2. Von der Linde D., Sokolowski-Tinten K., Bialkowski J. *Appl. Surf. Sci.*, **109-110**, 1 (1997).
3. Salle B., Gobert O., Meynadier P., Perdrix M., Petite G., Semerok A. *Appl. Phys. A*, **69**, S381 (1999).
4. Klimentov S.M., Garnov S.V., Kononenko T.V., Konov V.I., Pivovarov P.A., Dausinger F. *Appl. Phys. A*, **69**, S633 (1999).
5. Klimentov S.M., Kononenko T.V., Pivovarov P.A., Garnov S.V., Konov V.I., Prokhorov A.M., Breitling D., Dausinger F. *Kvantovaya Elektron.*, **31**, 378 (2001) [*Quantum Electron.*, **31**, 378 (2001)].
6. Braun A., Korn G., Liu X., Du D., Squier J., Mourou G. *Opt. Lett.*, **20**, 73 (1995).
7. Krushelnick K., Ting A., Moore C.I., Burris H.R., Esaray E., Sprangle P., Baine M. *Phys. Rev. Lett.*, **78**, 4047 (1997).
8. Nisoli M., Stagira S., De Silvestry S., Svelto O., Sartania S., Cheng Z., Lenzner M., Spielmann Ch., Krausz F. *Appl. Phys. B*, **65**, 189 (1997).
9. Sarkisov G.S., Bychenkov V.Yu., Novikov V.N., Tikhonchuk V.T., Maksimchuk A., Chen S.Y., Wagner R., Mourou G., Umstadler D. *Phys. Rev. E*, **59**, 7042 (1999).